Journal of Structural Biology **135,** 281–293 (2001)
doi:10.1006/jsbi.2001.4413, available online at http://www.idealibrary.com on IDEAL®

The Quaternary Arrangement of HslU and HslV in a Cocrystal: A Response to Wang, Yale

Matthias Bochtler,*,†,[1] Hyun Kyu Song,‡ Claudia Hartmann,‡ Ravishankar Ramachandran,‡ and Robert Huber‡

**International Institute of Molecular and Cell Biology, ul. Ks. J. Trojdena 4, 02-109 Warsaw, Poland; †Max-Planck-Institute of Molecular Cell Biology and Genetics, Pfotenhauerstr. 108, D-01307, Dresden, Germany; and ‡Max-Planck-Institut für Biochemie, Am Klopferspitz 18a, D-82152 Martinsried/Planegg, Germany*

Received July 16, 2001, and in revised form September 8, 2001; published online November 13, 2001

Protease HslV and ATPase HslU form an ATP-dependent protease in bacteria. We have previously determined the structure of the components of this protease. In the case of HslU, the structure was derived from HslU–HslV cocrystals, combining phase information from MAD and the previously determined HslV model. Whereas the structures of the components were confirmed in detail by later structures, the quaternary arrangement of HslV and HslU was not reproduced in later crystal forms. In a recent communication to this journal, Wang attempted a reinterpretation of our original data to account for this difference. In response, we demonstrate that difference Pattersons, difference Fouriers, molecular replacement calculations, *R* factors, and omit maps all support our original analysis and prove that the suggested reinterpretation is false by these criteria. In particular, we show that our crystals are essentially untwinned and that only the originally reported quaternary arrangement of HslV and HslU particles is consistent with the experimental data. We finally demonstrate that Wang's newly introduced R_{tpart} method to predict translational corrections for a subset of the unit cell contents is systematically flawed.

INTRODUCTION

The ATP-dependent bacterial protease HslVU (Missiakas *et al.*, 1996; Rohrwild *et al.*, 1996, 1997) has attracted a lot of interest in recent years as a model system for the eukaryotic proteasome. HslVU is a fairly labile complex and does not survive most chromatographic procedures. It is therefore easy to purify the components separately. A number of years ago we solved the structure of *Escherichia coli* HslV, the proteolytic core of this protease, by MIR from crystals that contained HslV only (Bochtler *et al.*, 1997). Unlike eukaryotic proteasomes, which form complexes of sevenfold or pseudosevenfold symmetry, HslV is a dimer of hexamers and forms a central proteolytic cavity with threonine nucleophiles on the interior walls of the particle. The structure of HslV was the starting point for the structure determination of HslU by MAD from crystals that contained both HslV and HslU particles (Bochtler *et al.*, 2000). HslU, classified originally only as an Hsp100 protein, turned out to be a member of the AAA(+) family of ATPases with N- and C-domains that are typical of AAA proteins. A sequence insertion unique for HslU among Hsp100 proteins turned out to be a labile helical coiled coil structure and was termed the I-domain (see Fig. 1b). The original structure of the HslU hexamer (PDB Accession Code 1DOO) was soon superseded by an almost identical structure of HslU in the same crystal form (PDB Accession Code 1E94), but for a crystal grown in the presence of casein that yielded a cleaner diffraction pattern (Song *et al.*, 2000). These structures of HslU were confirmed to high accuracy by ourselves in two independent crystal forms of HslU (Bochtler *et al.*, 2000) (PDB Access Codes 1DO0 and 1DO2) and later also by other groups with the *H. influenzae* enzyme (PDB Accession Code 1G3I) (Sousa *et al.*, 2000) and the *E. coli* enzyme (PDB Accession Codes 1G4A and 1G4B) (Wang *et al.*, 2001). Wang had been unable to obtain independent phase information and applied molecular replacement using our models. With the exception of two surface loops and the flexible I-domain, which was not seen by Wang *et al.*, the later two structures of the *E. coli* enzyme confirm our original structures in full detail (see Fig. 1).

In contrast to the structures of the components,

[1] To whom correspondence and reprint requests should be addressed at International Institute of Molecular and Cell Biology, ul. Ks. J. Trojdena 4, Warsaw 02-109, Poland.

1047-8477/01 $35.00

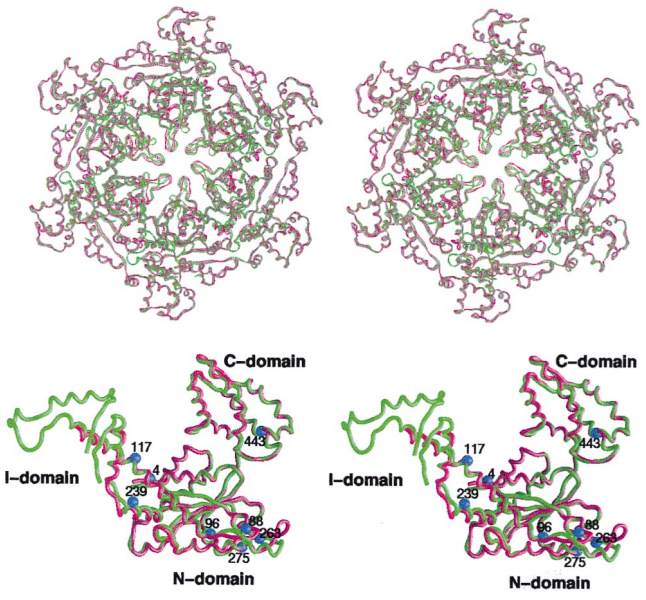

FIG. 1. Superposition of the original HslU structure (1DOO, green) with Wang's later version (1G4A, red). With the exception of a surface loop at the particle entrance (that was not seen by Wang), the later structure is almost identical with our original structure. The rmsd is 1.4 Å for all matching Cα atoms and 0.6 Å for a total of 301 matching Cα atoms (residues 4–88, 96–117, 239–263, 275–443). The figure was drawn with GRASP (Nicholls, 1992).

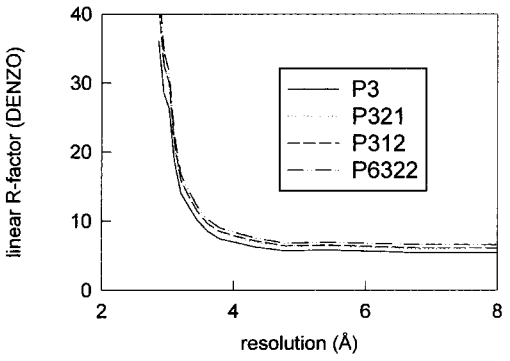

FIG. 2. Data reduction statistics for the various possible space groups. The linear *R* factor as output by DENZO is plotted as a function of resolution. The curves run almost in parallel, indicating true Patterson symmetry P6/mmm.

the quaternary arrangement of HslU and HslV in our HslV–HslU cocrystals is at variance with other experiments. EM images (Ishikawa *et al.*, 2000; Rohrwild *et al.*, 1997) and later X-ray structures (Sousa *et al.*, 2000; Wang *et al.*, 2001) show a docking mode between HslU and HslV with the I-domains distal to HslV. This docking mode has also been termed ASMS (apical surface-mediated structure). In contrast, our original structure shows an

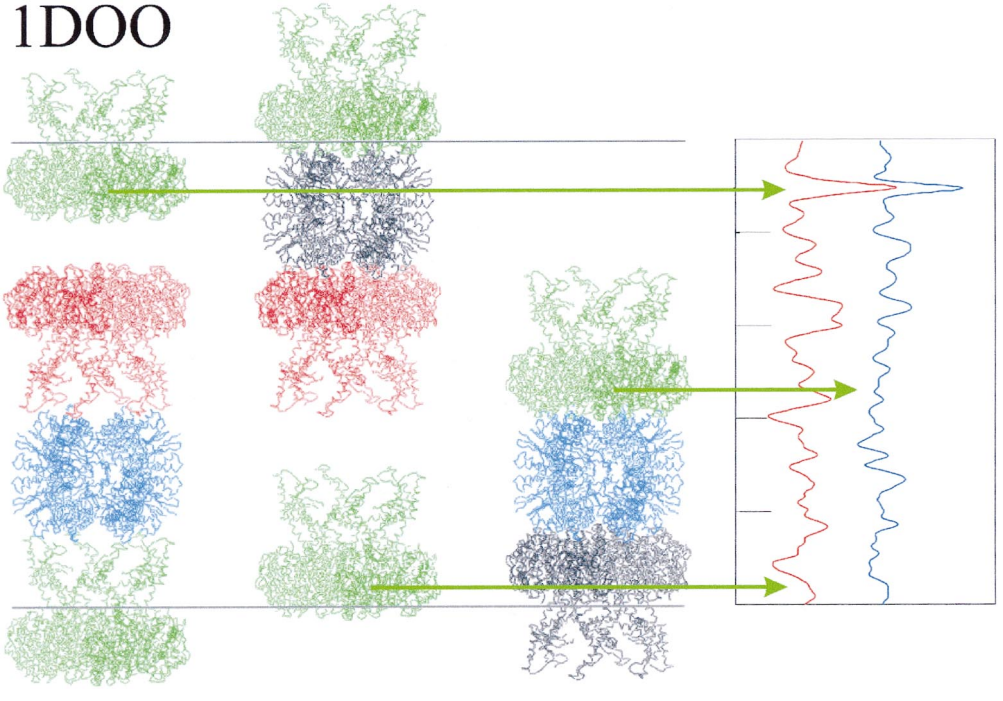

FIG. 3. Arrangement of HslU (red and green) and HslV (blue) on a crystallographic threefold axis. The panel on the very left shows the originally reported arrangement. The *c* axis runs vertically, and the horizontal lines delimit one unit cell. In a first experiment, the HslU particle with I-domains down (red) was fixed and the HslU particle with I-domains up (green) was translated in the *z* direction. The red trace in the rightmost panel shows the MR signal, and the horizontal green lines point to the expected location of peaks for the two arrangements. In a related experiment, HslV (blue) was fixed and HslU with I-domains up (green) was translated. The blue trace shows the result, and green horizontal arrows again indicate the expected location of peaks. Both experiments confirm the original interpretation.

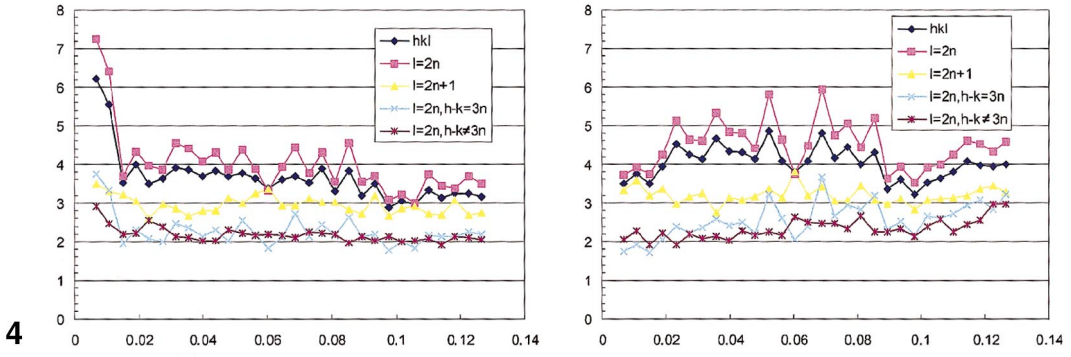

4

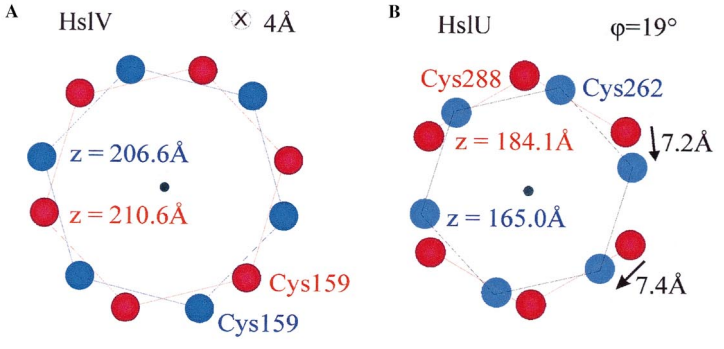

5

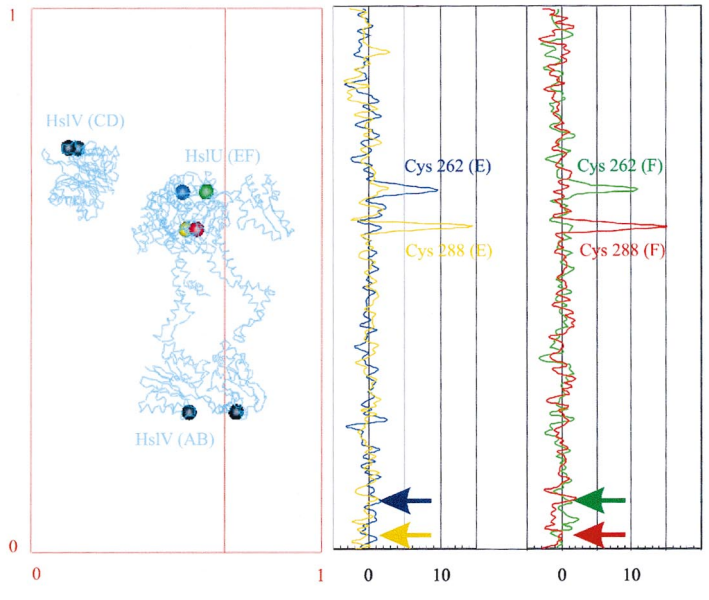

6

FIG. 4. Wilson ratios as calculated on the basis of the original molecular model (left) and the experimental data (right) as a function of the squared inverse resolution in $1/Å^2$. This way of plotting the data assures that the same number of reflections contributes for every resolution shell. We fail to find the systematic 70% deviation reported by Wang.

FIG. 5. View of the heavy atom sites of HslV and HslU along the sixfold axis. In (A), the two rings of heavy atoms on HslV (red and blue) are 4 Å apart. In (B), the two planes of heavy atoms (red and blue) are a full 19 Å apart. A rotation of around 20°, equivalent to a lateral shift of more than 7 Å, is required to introduce inversion symmetry into the assembly.

FIG. 6. View of the (110) plane of the direct lattice, with the Cα trace of the asymmetric unit drawn in blue. Heavy atoms are indicated in the originally assigned positions, with heavy atoms on HslV indicated in black and heavy atoms on HslU drawn in blue, green, yellow, and red. In the left panel, we have plotted the anomalous difference Fourier on lines through our heavy atom positions. In all cases, we find clear signals for the originally assigned positions and no signals at the sites predicted by Wang and indicated by the arrows.

arrangement with the I-domains proximal to HslV, a mode of docking which has also been called DIMS (domain-I-mediated structure). After extensive molecular replacement calculations, HslU–HslV cocrystals were assigned to space group $P6_322$ in spite of imperfect extinctions along the *c* axis. We find free particles of HslV on (0, 0, 1/4) and (0, 0, 3/4) (Wyckoff positions *2b*, site symmetry 3.2) that can be built up from two crystallographically independent subunits that we termed C and D. In addition, there are HslV particles on threefold axes at (1/3, 2/3, 1/4) and (2/3, 1/3, 3/4) (Wyckoff positions *2c*, site symmetry 3.2). In $P6_322$, these particles can be built up from two independent subunits that we termed A and B. These particles alternate with HslU particles on the crystallographic threefold axes (Wyckoff positions *4f*, site symmetry 3..). In $P6_322$, only two HslU subunits are crystallographically independent. They were termed E and F.

In a communication to this journal, Wang recently suggested that the reported DIMS arrangement of HslU and HslV particles was due to a crystallographic error rather than to the balance between physiological HslU–HslV interactions and crystal packing forces (Wang, 2001). Specifically, Wang questions the Patterson symmetry, the assignment of a screw axis, and, most importantly, the consistency of crystallographic origins (Wang, 2001). Furthermore, he introduces R_{tpart} as a new structure validation tool in support of the suggested shift of origin (Wang, 2001).

In response to this communication, we first present the original R_{merge} data to support the originally assigned Patterson symmetry 6/mmm. We continue with a demonstration that interparticle cross-vectors between HslU particles on the same axis and between HslU and HslV particles on the same axis predict the originally reported DIMS arrangement and are not compatible with the presence of ASMS in our data. Although this result would remain valid in the presence of twinning, we next show with Patterson search techniques that twinning is essentially absent in our HslV–HslU complex crystals, since both sets of dyads perpendicular to the *c* axis are crystallographic axes and not twinning axes. Contrary to Wang's statements, Wilson ratios are consistent with this conclusion. We continue to show that the originally assigned mercury positions were on the same crystallographic origin, as shown with a very clear signal in difference Fouriers, a conclusion that is also supported by the analysis of difference Pattersons. Finally, we demonstrate that unlike R_{part}, the newly introduced R_{tpart} (Wang, 2001) is not suitable as a structure validation tool, because it predicts shifts that depend on the method and not on the molecular model.

METHODS

Programs

Data were recorded on CCD detectors (Ta and Hg derivatives, native dataset 1E94) and on an MAR345 image plate (native dataset 1DOO). Data integration was done with DENZO, and merging and scaling were done with SCALEPACK (Otwinowski and Minor, 1997). All other calculations were done with programs of the CCP4 suite (CCP4, 1994). F_{calc}s and φ_{calc}s were calculated with SFALL, figures of merit for phases with SIGMAA, and Fouriers, difference Fouriers and Pattersons with FFT. Real and cross-vector searches were done with RSPS. Molecular replacement calculations were done with CCP4 AMORE at 4.5 or 5.0 Å resolution. Full models of HslV and HslU particles were used, although this usually covered more than the asymmetric unit. The advantage of this procedure is that known intersubunit vectors within one HslV or HslU particle contribute to the molecular replacement signal. This increases the signal to noise ratio for both rotational and translational searches. All translation searches were done with Crowther and Blow (1967) translation functions.

Comparison of Molecular Replacement Signals

For a direct comparison of molecular replacement signals from the original DIMS complex and from Wang's ASMS arrangement, we have built up the original DIMS complex from components of Wang's structure 1G4A. This precaution excludes bias for DIMS from previous refinement of the complex against the experimental data. For comparison, we have symmetrized Wang's singly capped HslVU species 1G4A, applying the local twofold symmetry in HslV. The 1G4A was chosen to build up the ASMS complex, as this complex is the only ASMS complex that can be generated from the original DIMS complex with a simple shift without rotation (see below). To work with equal numbers of atoms, I-domains were omitted. Calculations were done both in P3 and in $P6_322$. As both arrangements share a large set of self-vectors, they both give clear rotational solutions, which can be used as input for translational searches.

Patterson Methods in the Presence of Twinning

The advantage of Patterson searches over other methods to place known molecules in an unknown crystal is their applicability in the presence of twinning. This well-known property of Pattersons is based on the simple fact that summations and Fourier transforms commute. Assume that a twinned crystal *S* contains single crystals *A* and *B* related through twinning operation *T*. Thus, diffraction intensities from *S* are diffraction intensities from *A* added to diffraction intensities from *B*. Therefore, if the Patterson of *S* is calculated in a straightforward way (disregarding twinning), one obtains the sum of Pattersons from *A* and *B*. Thus, the Patterson still contains all peaks from crystal *A* (and of course *B*) in the presence of twinning. A molecular model for *A* (or *B*) that predicts Patterson vectors that are not observed in the Patterson is therefore excluded regardless of whether twinning is present.

Next, we demonstrate that the naive calculation of anomalous difference Pattersons (disregarding twinning) yields *on average* the Patterson that would be obtained for the heavy atoms in the twinned crystal in the absence of protein. This result is less straightforward than it sounds and requires some additional assumptions, since anomalous difference Pattersons are calculated from squares of *amplitude* differences. Assuming that anomalous amplitude differences are small compared to amplitudes, it can be shown (for 50–50% twinning) that

$$S^+ - S^- = (F_A^+ - F_A^-)\,\frac{F_A}{S} \pm (F_B^+ - F_B^-)\,\frac{F_B}{S},$$

where S^+ and S^- are the naively calculated structure factors for the twin, S is the average of S^+ and S^-, and F_A^+ and F_A^- are

Friedel mates for true single crystal A and F_B^+ and F_B^- are Friedel mates for true single crystal B, where it is assumed that F_A and F_B contribute to the same reflection, i.e., $F_S^2 = F_A^2 + F_B^2$. Let $F_{A,\mathrm{H}}$ and $F_{B,\mathrm{H}}$ denote the magnitudes of the anomalous scattering components of the heavy atoms, α_H and β_H the geometric phases of the heavy atom scatterers, and let α_P and β_P denote the phases for all nonanomalous scattering, including nonanomalous scattering from the heavy atoms in crystals A and B. Then the usual approximation $(F_A^+ - F_A^-) = 2\,F_{A,\mathrm{H}}\sin(\alpha_\mathrm{P} - \alpha_\mathrm{H})$ applies for A and correspondingly for B. In general, the magnitudes of amplitudes and amplitude differences are not correlated, and protein and heavy atom phases are not correlated either. Thus, on average

$$(S^+ - S^-)^2 \propto (F_A^+ - F_A^-)^2 + (F_B^+ - F_B^-)^2.$$

This means that if twinning is present and Patterson vectors are calculated in a naive way (with no corrections for twinning), one obtains a Patterson that is similar to the Patterson from the twinned heavy atom structure alone.

RESULTS AND DISCUSSION

Laue Group Assignment

HslVU crystals are trigonal, with lattice constants of roughly 172 Å/172 Å/278 Å. Crystals planes perpendicular to the c axis look nearly perfect. In contrast, crystal faces parallel to the c axis appear somewhat rough and layered. On in-house rotating anode generators, the smear of diffraction spots in the c direction is usually prohibitive for data collection. With the much finer beam at synchrotrons, the situation improves dramatically, and data to 2.8 Å with apparent Patterson symmetry P6/mmm can be recorded. It was recently suggested by Wang that the true symmetry of the Patterson is in fact lower than P6/mmm. This suggestion can be tested from the shape of the plot of R_{merge} as a function of resolution. Any symmetry elements that are not true Patterson symmetries should increase R_{merge}, particularly at low resolution, where measurement errors are small. Conversely, if R_{merge} curves for lower and higher symmetry run in parallel, this argues for the presence of the higher symmetry. This is precisely what we observe for our data (dataset 1E94, P3 data submitted to PDB, see Fig. 2). At this stage, the presence of any symmetry element in Patterson space can of course be attributed either to crystallographic symmetry or to perfect (50–50%) hemihedral twinning. An extreme case would be perfect twinning around both sets of nonequivalent twofold axes (i.e., $h, k, l \rightarrow h - k, -k, -l$ or $h, k, l \rightarrow -k, -h, -l$). As the strong–weak pattern along the 00l line excludes 3_1, 3_2, 6_1, 6_2, 6_4, and 6_5 screw axes along c, the space group has to be P3, P321, P312, P6, P6_3, P622, or P$6_3$22. Since P3 is a subgroup for all these possibilities, calculations in P3 are valid irrespective of the final space group assignment.

Patterson Vectors Are Compatible with DIMS, but Not with ASMS

In P3, Patterson cross-vectors between crystallographically related HslU or HslV particles fix the location of these particles perpendicular to the c axis. In contrast, the arrangement along the c axis depends exclusively on the docking mode between the two particles. Thus, the correlation between predicted Patterson cross-vectors and the observed Patterson can be used to distinguish the two docking modes.

To exclude any bias for DIMS from previous refinement of our HslV and HslU models against the diffraction data, we used HslV and HslU from 1G4A (Wang *et al.*, 2001) for all calculations. Rotation functions were calculated at 4.5 Å with the full HslV dodecamer and the HslU hexamer as search models (radius of integration 40 Å). As expected, we found one set of equivalent solutions for HslV (signal 27.4, highest noise peak 21.6) and two sets of equivalent solutions for HslU. These represent HslU particles with I-domains up (signal 30.0, highest noise peak 23.3) and I-domains down (signal 29.4, highest noise peak 23.3).

We proceeded to calculate cross-translation functions for HslU with I-domains up (green in Fig. 3). In the first experiment, we fixed HslU with I-domains down (red in Fig. 3) at the height where it is located in P$6_3$22 (thus defining the origin in P3) and calculated a cross-translation function to locate HslU with I-domains up. The red trace in Fig. 3 shows the signal on the (1/3, 2/3, z) line as a function of z. We found a strong peak consistent with the original position at $z = 0.90c$. This peak is the highest peak in full three-dimensional searches. Since Wang's reinterpretation requires a shift of HslU by $0.57c$ for fixed HslV, it is easily seen that his analysis predicts a peak at $(0.90c + 2*0.57c) = 2.04c$ or $0.04c$. No such peak was observed, excluding the presence of ASMS in our data.

Next, we tested whether a singly capped HslVU species ($U_6V_6V_6$) with I-domains distal to HslV could be compatible with our data. Proceeding as in the previous experiment, we fixed one HslV particle (blue in Fig. 3) at the height where it is located in P$6_3$22 (thus defining the origin in P3). Once more, we calculated a cross-translation function to locate HslU with I-domains up (green in Fig. 3). The blue trace in Fig. 3 shows the signal on the (1/3, 2/3, z) line. Again, a strong peak confirmed the original HslU location at $z = 0.90c$. In contrast, there was no signal at $0.90c + 0.57c = 1.47c$ or $0.47c$, disproving once more Wang's reanalysis.

In summary, Wang's assumption of ASMS in our crystal predicts Patterson vectors that are not found in experimental Patterson maps. It is therefore

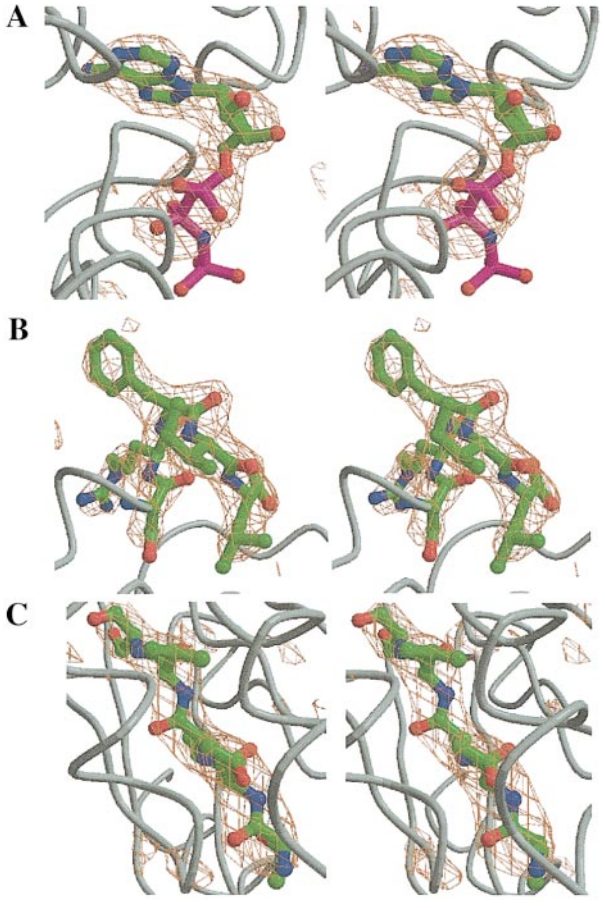

FIG. 7. Stereo diagrams of Fo-Fc-simulated annealing omit maps at 3σ of (A) the ATP binding site of HslU, (B) the C-terminal segment (five residues) of HslU, and (C) the N-terminal segment (five residues) of HslV. Omitted residues are drawn in ball and stick representation; for all other residues, only the Cα trace is shown. This figure was drawn with BOBSCRIPT (Esnouf, 1999) and rendered with RASTER3D (Merrit and Bacon, 1997).

ruled out, whereas the original analysis is confirmed. This argument remains valid in the presence of twinning, since twinning can introduce spurious Patterson vectors from the twinning mate, but cannot possibly eliminate Patterson vectors. A more detailed account of this argument is given under Methods.

The Patterson Symmetry P6/mmm Is Not Due to Twinning

Although Patterson searches are poor tools for discriminating between exact and approximate crystallographic symmetry, they are excellent tools for distinguishing between these two possibilities and twinning. This is what we set out to do.

Assume that the Patterson symmetry around both sets of twofold axes perpendicular to the *c* axis is due to twinning. In this case, no cross-vectors between particles that would be related through crystallographic axes in the higher symmetry space groups should be present. Consequently, cross-vector searches in the higher symmetry space groups should fail to pinpoint the location of molecular models along the *c* axis. Conversely, if these searches yield high signals and position the molecules in a way that is consistent with cross-vector searches between crystallographically unrelated objects, this proves that the dyads perpendicular to the *c* axis are not due to twinning.

We started from the assumption that the crystallographic symmetry in our crystals is P3 or higher. To prove that it is P312 or higher, we attempted to place one particle of HslU (with I-domains up) in the unit cell. If the dyads in apparent "P312" were due to twinning, the expected cross-vectors between HslU and a crystallographic symmetry mate that allow us to locate the particle in the *c* direction would be missing in experimental Patterson maps. Thus, failure to position a particle of HslU (or HslV) in P312 would demonstrate that the dyads are twinning axes. Conversely, successful placement consistent with HslV–HslU cross-vector searches (and thus with the original packing) demonstrates that the dyads are true symmetry axes. In practice, HslU was subjected first to a rotation search, resulting in the top solution for HslU with I-domains up. This orientation was then used for a translation search (see Table Ia). The top solution with a very clear signal to noise ratio (30.3 to 24.7) is (1.000, 1.000, 0.1463). In P312, this is equivalent to (0.333, 0.667, 0.6463). Since the conventional unit cell for P312 is shifted 0.25 upward in the *c* direction with respect to the conventional unit cell for $P6_322$, this is equivalent to our previously reported AMORE solution (0.333, 0.666, 0.896) that represents the originally reported packing in $P6_322$. Thus, the dyads in P312 are true symmetry axes.

Next, we proceeded in an analogous manner to demonstrate that the symmetry of our crystals is P321 or higher. Again, we attempted to place one particle of HslU in the unit cell. The result is shown in Table Ib. The second best solution is equivalent to our previously reported solution (0.333, 0.666, 0.896). This proves that the second set of twofold axes is again not merely due to twinning. The top peak in Table Ib arises from a complication due to the sixfold symmetry of HslU. Due to this local sixfold (twofold) axis, placing a particle at (1.000, 1.000, 0.1463) in P321 predicts the same set of Patterson vectors as placing the particle at (1.000, 1.000, 0.1463) in P312. Consequently, this top peak can be taken as further confirmation that the space group is P312 or higher.

The presence of Patterson vectors for both sets of dyads strongly suggests that the space group is P622 or $P6_322$, as the two sets of twofolds can be either in

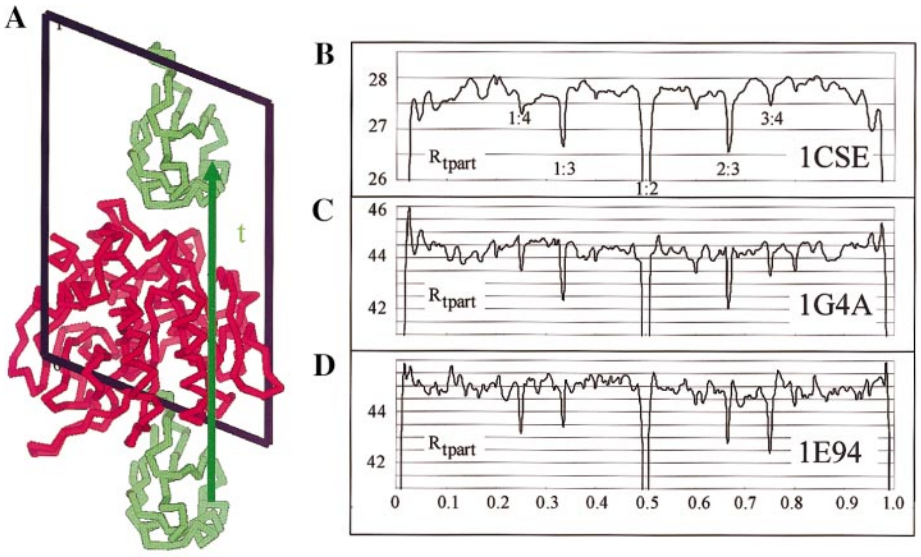

FIG. 8. (A) This illustrates the calculation of R_{tpart} according to Wang. Part of the unit cell contents (drawn in green, eglin C in the example) is translated by t, whereas the rest (drawn in red, subtilisin Carlsberg in the example) is fixed. Then the R factor for the shifted model is calculated, treating calculated structure factors of the original model as the reference. In the panel on the right, trace B shows the calculated R_{tpart} for fractional shifts between 0 and 1. The function has minima at small fractional numbers. The same is true if the method is applied to Wang's HslU–HslV cocrystals (1G4A, trace C) and to our HslV–HslU cocrystals (1E94, trace D).

the same plane (P622) or shifted by 1/4 in the c direction ($P6_322$). P622 inevitably places HslU particles on threefold (or sixfold) crystallographic axes. For all possible rotations of HslU around this axis, the radius of HslU is too large to allow packing in the ab plane. For the correct azimuth of HslU, the particles interpenetrate by about 20 Å. Even if arbitrary rotations of HslU around the sixfold crystallographic axis are allowed, the particles continue to overlap (data not shown). With space group P622

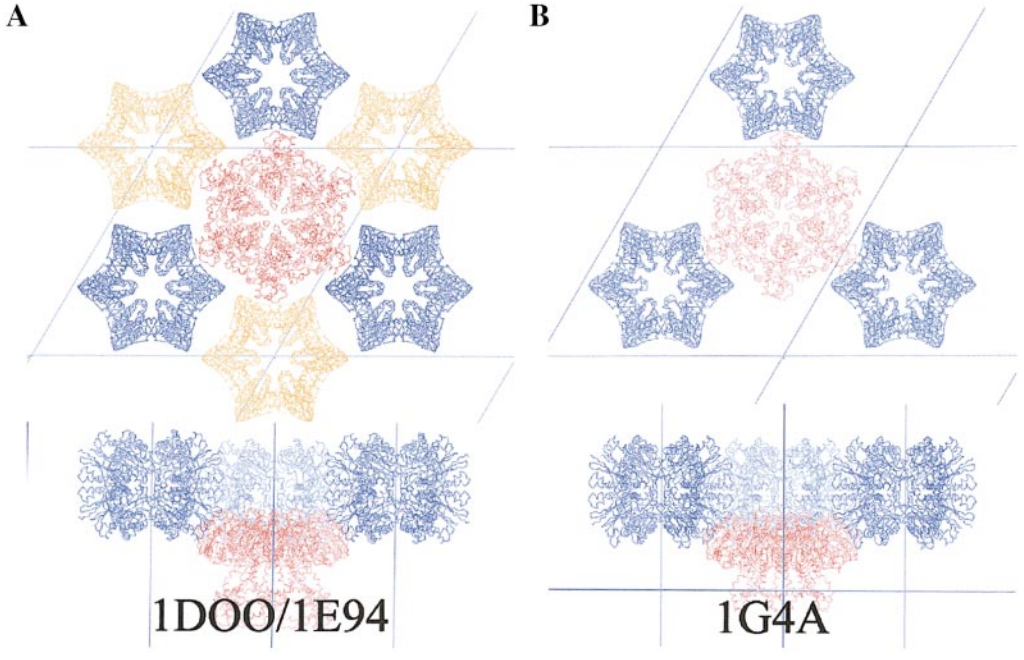

FIG. 9. Identical lateral packing in our HslV–HslU cocrystals and in Wang's 1G4A crystals. The top panels show views along the z axis; the bottom panels are views perpendicular to the z axis. HslV particles generated from independent subunits A and B (blue) in 1DOO play analogous roles to the HslV particles (blue) of 1G4A and fix the orientation of HslU (red). To emphasize this point, the free HslV particles in 1DOO (brown) have been omitted in the side view (left, bottom panel).

TABLE I
Predicted HslU Positions in Space Groups P312 and P321

(a) P312				(b) P321			
x	*y*	*z*	Height	*x*	*y*	*z*	Height
1.000	1.000	0.146	30.3	1.000	1.000	0.146	30.1
0.000	1.000	0.496	24.7	0.333	0.667	0.396	26.5
1.000	1.000	0.000	24.4	0.667	0.333	0.396	26.4
1.000	1.000	0.020	23.8	1.000	1.000	0.496	24.8
1.000	1.000	0.418	23.8	0.667	0.333	0.2474	24.8

Note. The top peak in (a) and the top two peaks in (b) are consistent with our packing. This demonstrates that the dyads are not mere twinning axes.

ruled out, the only remaining possibility is space group $P6_322$.

We point out that the above calculations not only support the presence of the two sets of dyads perpendicular to the *c* axis in single crystals of HslU–HslV, they also confirm once more the original placement of HslU and disprove Wang's reinterpretation of our data.

The Packing of $P6_322$ Can Be Built Up in P3 by Molecular Replacement

Although the above arguments would generally be regarded as sufficient to prove that both sets of dyads perpendicular to the *c* axis are crystallographic, the special packing in our crystals could be taken as an argument that the dyads in our crystal are local axes only that happen to be located in special positions. Thus, one could suspect a scenario in which only part of the unit cell would follow true $P6_322$ symmetry. In this case, a single crystal would have lower symmetry, and the observed P6/mmm Patterson symmetry would be ascribed to twinning. To exclude this scenario, we have attempted to build up the $P6_322$ unit cell by molecular replacement in P3. This is indeed possible, starting with the placement of one HslU particle (the origin has to be fixed consistently with $P6_322$), followed by placement of another HslU particle in the opposite orientation, and finally by placement of the HslV particles. In all cases we find that the top-scoring solutions are the ones that are expected from the original packing in $P6_322$ (data not shown, available from the authors on request).

A Direct Comparison of the Original Interpretation with Wang's Reinterpretation

We finally calculated rotation and translation functions of our model and of Wang's reinterpretation in both P3 and $P6_322$, again assembling both our and Wang's complex from Wang's components. In P3, AMORE failed to find a translational solution for Wang's complex, but yielded our original solution as the only peak (30% correlation, next highest peak 7%) if the DIMS complex was used as the search model. If calculations were done in space group $P6_322$ (with the contents of the P3 asymmetric unit), the top-scoring solution for the originally reported DIMS arrangement had 69% correlation compared to 50% for the ASMS arrangement. Inspection shows that the top solution for DIMS is our originally reported arrangement. The top solution for ASMS corresponds to the solution suggested by Wang with complete $U_6V_6V_6U_6$ particles at (1/3, 2/3, −1/4) and (2/3, 1/3, 1/4). Apparently, Wang did not notice that this solution is ruled out not only by the very substantially lower correlation coefficient, but also by severe molecular overlap, involving an interpenetration of $C\alpha$ traces to a depth of at least 10 Å. Finally, the ASMS solution is ruled out by its prohibitively high *R*-factor of 48% after bulk solvent correction (Wang, 2001). Although this solution fails to predict the correct set of cross-vectors between crystallographically related HslU particles, it does account for cross-vectors between crystallographically related HslV particles that are identically placed as in the original, correct packing and therefore appears as the top score in searches with ASMS as the search model.

Wilson Ratios Do Not Suggest Twinning

The Wilson ratio (i.e., $\langle I^2\rangle/\langle I\rangle^2$) is a measure of the spread in intensity (over many reflections) relative to the average intensity. In statistical terms, it can be expressed as $1 + (\sigma/\mu)^2$, where σ and μ are the spread and average value of the intensity. Formulated in this way, it is immediately clear that the Wilson ratio is expected to be lower in twinned crystals, since the extremes of intensity tend to be averaged out by the twinning operation. For a crystal without local symmetry, the intensity for any particular (acentric) reflection can be treated as the result of a random walk in complex structure factor

space. In this case, the mathematics predicts a Wilson ratio of 2 for an untwinned crystal and a value of 1.5 for a twinned crystal. This is the well-known twinning criterion (Yeates, 1997). It does not apply for crystals where the packing enforces systematic strong–weak patterns in reciprocal space. In this case, the spread in intensities, and thus the Wilson ratio, is systematically larger than for crystals without local symmetry.

In the case of our HslU–HslV crystals, it can be shown that reflections with $l = 2n + 1$ and $h - k = 3n$ would be extinct if local symmetry was perfect. Conversely, reflections with $l = 2n$ and $h - k = 3n$ are expected to be particularly strong. For this subset of reflections, partial structure factors of all four HslV particles (in P1) have the same phase. The same is true of HslUs with identical orientation. Thus, the spread in intensities for all hkl is larger than expected on the basis of random walk experiments.

To make the argument quantitative, we have used our original HslV–HslU model to calculate expected Wilson ratios for hkl and for the four zones suggested by Wang. Contrary to Wang's statements, the results (left panel of Fig. 4) compare favorably with experimental data (right panel of Fig. 4). We draw particular attention to the zone $l = 2n$, $h - k = 3n$. For this zone, and assuming perfect local symmetry, our crystal scatters as a P1 crystal with one particle of HslV of occupancy 4 and with two particles of HslU (with I-domains up and down) of occupancy 2. Thus, for this zone, the crystal behaves as if no special translations were present. As a result, classical Wilson statistics apply for this zone, and indeed the expected value of 2 for an untwinned crystal is observed. Thus, disorder in the c direction in our crystals does not represent classical twinning.

Partial Model Phases and Mercury Heavy Atom Sites Are Not Centrosymmetric

It is a well-known pitfall that spurious heavy atom sites are found if a centrosymmetric set of heavy atoms is used to phase difference Fouriers to identify additional heavy atom sites. In the absence of an anomalous signal, the resulting difference Fourier maps are centrosymmetric (with respect to the inversion center (x_0, y_0, z_0) of the original set of heavy atoms). SIR maps that are calculated from a centrosymmetric set of heavy atoms suffer from the same problem. In both cases, the phases can be expressed as $\alpha_{hkl} = 2\pi(hx_0 + ky_0 + lz_0) + \pi/2 \pm \pi/2$, a condition that Wang refers to as "centrosymmetry of the phases." It appears that the approximate centrosymmetry of a set or subset of assumed mercury heavy atom sites in our structure (the original mercury data were not available to him) led Wang to suspect similar problems in our structure.

In response, we point out that the clue to structure determination of the HslU–HslV crystals was the placement of one particle of HslV (of 622-point symmetry) on a crystallographic position of 32-point symmetry. These phases (and not phases from any set of heavy atoms) were subsequently used to locate heavy atom positions in anomalous difference Fourier maps. This procedure assures a common crystallographic origin for all heavy atom sites.

Wang's argument that phases from the partial model "still possess the centrosymmetry originating in the amplitudes" (Wang, 2001) is incorrect and easily disproven. As the initial HslV model contains L amino acids, phases from this model are surely not centrosymmetric. The subsequent sigmaa procedure (CCP4, sigmaa, mode partial) to obtain figures of merit for these phases leaves the phases themselves untouched (the phases from the partial model represent the best guess). Thus, difference Fouriers are calculated with phases from the HslV model. Likewise, anomalous difference Fouriers are calculated from these phases after the usual 90° shift. Both sets of phases are therefore surely not centrosymmetric. Note that the relative scattering power of the partial model is entirely irrelevant for this argument. A model that represents a larger part of the total scattering mass will of course yield better phases. But these phases are in no way "less" centrosymmetric than phases from a very incomplete model.

Experiment supports this theoretical expectation. In the phase set for all reflections (including centric ones) calculated from the partial HslV model (chains A and B), phases differ on average by 40° from the expected values of 0° and 180° for a centrosymmetric set of phases (assuming the inversion center is at the origin). For a random phase set with only acentric reflections, the expected value is 45°. Thus, Wang's claim of centrosymmetry of the partial model phases is clearly not borne out by the data.

Wang's subsequent statement that "any derivative isomorphous (or anomalous) difference Fourier maps using these phases would actually be the difference Patterson maps" (Wang, 2001) is equally incorrect. First (difference) Patterson maps are Fourier transforms of squares of amplitudes (amplitude differences) with phases set 0. Second, and more importantly, the phases are neither centrosymmetric nor systematically 0. Any coincidences between Patterson peaks and peaks in difference Fouriers are therefore simply due to the fact that Patterson space is densely populated. It is telling that Wang found such coincidences also for HslV positions which he later declared correct (Wang, 2001).

Contrary to Wang's misquote of our work, neither the heavy atom sites on HslV nor the heavy atom sites on HslU are centrosymmetric. As shown in Fig.

5A, the two rings of heavy atoms bound to Cys159 on HslV are 4 Å apart. The deviation from centrosymmetry is even larger for the heavy atom sites on HslU. As shown in Fig. 5b, one ring of heavy atoms has to be rotated by approximately 20°, equivalent to a lateral shift of more than 7 Å. Moreover, the two alleged centers of inversion symmetry in HslV and HslU are inconsistent with each other.

The Mercury Sites Are on a Common Origin and Compatible only with Our Original DIMS Complex

Wang's allegation that our HslV–HslU structure was solved on inconsistent origins is incompatible with his suggested translational correction of the HslU component by $0.57c = 0.5c + 20$ Å. At 3 Å resolution, a shift of 20 Å corresponds to a phase shift of 2π for $l = 280/20 = 14$. Since the data are up to roughly $l = 50$, the additional 20-Å shift alters the phase of most reflections by more than 2π and is clearly no small adjustment. With Wang's reanalysis thus disproven, we next proceeded to support our original interpretation with additional computational experiments.

For a first experiment, we placed the HslV particles (chains A–D) in $P6_322$ and used the phases to calculate difference Fouriers for the mercury dataset for the three different measured wavelengths. We find our originally assigned heavy atom sites close to HslV Cys159 (chains A–D) and HslU Cys 288 (chain E, F) as the top six peaks at all wavelengths. At the wavelength at the absorption maximum, peaks 7 and 8 represent the binding sites on Cys262 (chains E, F) (see Table II). At other wavelengths, these two sites are harder to identify. To demonstrate that there is no signal for Wang's reassigned heavy atom sites, we proceeded to plot the difference Fouriers along lines through the mercury atoms bound to Cys288 E and F and to Cys262 E and F. In all cases, there is a very clear signal for the originally assigned positions and there is absolutely no signal for the "corrected positions" (see Fig. 6).

To further confirm the consistency of heavy atom sites, we next used only the supposedly misplaced HslU particles to phase anomalous difference Fouriers. If Wang's reinterpretation of our data was correct, we should at best be able to recover the mercury sites on HslU. In contrast to this prediction, we find all four sites on HslV Cys159 among the top six peaks in anomalous difference Fouriers at both the absorption maximum and above. The remaining two peaks among the first six peaks are always the mercury atoms bound to Cys288 HslU E and F. These statements also hold true for the remote wavelength if one noise peak is ignored (data not shown).

To make the argument independent of model phases, we next tried to locate heavy atom sites in difference Pattersons in $P6_322$. As expected, signals were substantially weaker than in difference Fouriers. Nevertheless, among the top six sites identified by RSPS, five represent the correct, originally assigned heavy atom positions at HslV B, HslV A, HslU F, and HslU E in this order (the HslU F peak is treated as two almost coincident, but nonidentical peaks by the program). Again, Wang's reassigned heavy atom positions are not observed.

To make the argument independent of the discussion on space group, we next attempted to locate heavy atoms with the space group taken as P3. Although anomalous data were 40% complete only for this space group, we could locate correct heavy atom sites on HslV A, B, C, and D and HslU F among the top 10 peaks in difference Fouriers phased with HslV only (data not shown).

Taken together, all these tests confirm that the heavy atoms were correctly assigned. We further pointed out above that Wang's claim of inversion symmetry in our heavy atom positions is not borne out by the experimental data. Wang failed to notice these discrepancies because he worked with putative, guessed heavy atom sites, as the experimental heavy atom data were not available to him.

The Data Can of course Be Evaluated in P3, P321, or P312 to Account for Residual Intensity in Odd 00l

Dealing with HslV–HslU crystals with smear in the *c* direction for several years, the residual inten-

TABLE II

List of the 10 Highest, Crystallographically Independent Maxima in an Anomalous Difference Fourier Map of the Mercury Derivative Phased with HslVs (Chains A, B, C, D) only

x	*y*	*z*	Height	Comment
0.370	0.542	0.257	24.34	Cys159 HslV (A)
0.495	0.704	0.258	22.40	Cys159 HslV (B)
0.038	0.160	0.743	16.20	Cys159 HslV (C)
0.165	0.126	0.743	15.71	Cys159 HslV (D)
0.367	0.567	0.593	15.21	Cys288 HslU (F)
0.233	0.533	0.594	14.49	Cys288 HslU (E)
0.416	0.600	0.662	11.06	Cys262 HslU (F)
0.266	0.519	0.662	9.71	Cys262 HslU (E)
0.970	0.869	0.908	6.98	Not assigned
0.969	0.868	0.406	5.23	Not assigned

Note. The anomalous difference Fourier map was calculated in $P6_322$ at full resolution (3.0 Å), using the data at the absorption maximum. The map was normalized to put peak heights on an absolute scale. A full unit cell was searched for peaks. Among crystallographically equivalent heavy atom sites, the one attached to the polypeptide chain in the asymmetric unit of 1DOO was chosen. The assigned eight heavy atom positions correspond to the eight highest peaks in the list. The top two nonassigned peaks are also indicated.

sity of odd 00l spots in the *c* direction appeared to us as a natural result of crystal disorder in this direction (see Introduction). In fact the intensity in odd reflections is very small compared to the intensity in even reflections (total intensity in even reflections: total intensity in odd reflections = 12:1). Further, we were of course aware that odd extinctions in 00l were merely indicative of a $c/2$ periodicity of the projection of density on the *c* axis and could never prove the presence of the 2_1 (6_3) screw axis along *c*. Final proof or disproof of the presence of the screw axis is therefore only provided by successful structure determination. In protein crystallography, molecular replacement is commonly used to establish the nature of screw axes (most typically to distinguish between right- and lefthand screws, e.g., 6_1 and 6_5). We have established the presence of the screw axis by all these criteria, as shown in short by the *R* values (R_{cryst} = 25.4%, R_{free} = 30.4%) and by omit maps (see Fig. 7). Technically, it is of course possible to account for the residual intensity in odd 00l reflections by expanding the data to the asymmetric unit in P3 and refining against P3 data. This converts crystallographic symmetry into local symmetry and introduces extra degrees of freedom, which allow to lower R_{free} and R_{cryst}. This procedure merely improves crystallographic quality indicators (as does data evaluation in P1), but has no effect on the packing and the presence or the absence of DIMS or ASMS.

The New R_{tpart} Method Is Systematically Flawed

The R_{tpart} method (Wang, 2001) is designed to detect shifts in one component if two or more independent polypeptide chains are present in the asymmetric unit. Assume that the unit cells contains chains *X* and *Y*. According to Wang, systematic shifts of component *Y* can be detected by looking for minima in

$$R_{\mathrm{tpart}} = \sum_{h,k,l} |F_{calc,before} - F_{calc,after}| / \sum_{h,k,l} |F_{calc,before}|,$$

where $F_{calc,before}$ and $F_{calc,after}$ are structure factors calculated from the full model before and after shifting component *Y* by *t*. To simplify matters, the value of this function will first be assessed for space group P1.

Assume that the method is used to detect shifts along *c*. Assume further that *t* happens to be $c/2$. This means that for all reflections with even l, the partial structure factor from component *Y* is shifted in phase by a multiple of 2π, i.e, it is unchanged. Thus, for even l, it interferes with the partial structure factor from component *X* in exactly the same way as before the shift. Therefore, if summation of terms for R_{tpart} was limited to terms with even l, the R_{tpart} would be 0. If all terms are included, the result is nonzero, but still systematically small. Next, assume that the shift happens to be $+/-(m/n)*c$, where *m* and *n* are integers with no common divisor. This shift leaves the phase of the partial structure factor from *Y* unaffected for all l that are multiples of *n*. The larger *n*, the fewer the number of terms in the summation for R_{tpart} that are systematically 0. Still, such shifts lead to systematic minima. If crystallographic symmetry is present, special shifts of *Y* will translate into special shifts of its crystallographic symmetry mates. Thus, the situation is largely unchanged. R_{tpart} = 0 for 0 translation and will have minima for special translations, independently of the molecular model.

We have calculated R_{tpart} for a number of different PDB entries. The entry 1CSE, a complex of subtilisin with eglin C, represents the simplest case of a binary complex crystallized in space group P1 (one complex per unit cell). For the actual calculations, subtilisin was fixed and eglin C translated along the *c* axis (Fig. 8A). In P1, this is equivalent to fixing eglin C and moving subtilisin by $-t$. For every *t*, R_{tpart} was calculated. The result (Fig. 8B) confirms expectations. The minima for 0, 1/4, 1/3, 1/2, 2/3, 3/4 are clearly visible, although the simple theory does not explain why the minimum at $t = 1/2$ is so much more pronounced than the other minima. Next, we proceeded to calculate R_{tpart} for Wang's structure 1G4A in space group P321. Again, the same pattern is seen with minima for R_{tpart} at small fractional numbers (Fig. 8C). Finally, we applied the R_{tpart} method to 1E94, the DIMS HslVU complex (Fig. 8D). The trace shares all essential features with the trace for 1G4A, the ASMS complex.

We conclude that the essential features of the R_{tpart} trace are independent of the tested model. It is not surprising that R_{tpart} as a quality indicator that ignores observed data is not very useful. It is probably more surprising that R_{tpart} traces contain sharp features that are easily mistaken as properties of the tested model, especially if only a part of the curve that is permitted by packing is calculated.

A Retrospective on Wang's Paper

Being unaware of the smear of our diffraction patterns in the *c* direction, Wang was apparently intrigued by residual intensity in odd 00l reflections. We suspect that in addition to a reliance on his newly introduced R_{tpart} method, a series of misleading coincidences prompted him to suggest a twinning problem and a shift of origin in our structure:

Wang's crystals 1G4A (singly capped species, 167 × 167 × 161 Å, P321) and 1G4B (doubly capped species, 173 × 173 × 254 Å, P321) are both almost

perfectly merohedrally twinned (Wang, 2001) and happen to have cell constants that are related to the ones in 1E94 (172 × 172 × 277 Å, $P6_322$). This similarity of cell constants, especially between 1G4B and 1E94, apparently prompted Wang to suspect that our 1E94 crystals could be packed similarly to his 1G4B crystals and could suffer from related twinning problems. It appears to have escaped him that the 1E94 crystals have strong pseudoorigin peaks at (1/3, 2/3, 1/2) and (2/3, 1/3, 1/2) that are absent in 1G4B, ruling out any close similarity between the two crystal forms. We further point out that the diffraction powers of crystal forms 1E94 and 1G4B are very different (2.8 and 7.0 Å).

We suspect that Wang was prompted to suggest a shift of origin in our structure when he noticed that the azimuth of HslU relative to HslV in our structure matched the one observed in his singly capped HslVU complex structure (1G4A). We point out that this coincidence between the 1G4A and 1DOO/1E94 crystals (that differ in the *c* axis by more than 100 Å) is nicely explained by identical lateral packing (see Fig. 9). We further point out that the relative orientation of HslV and HslU is different in Wang's singly (1G4A) and doubly (1G4B) capped HslVU structures. If the HslV components of our DIMS complex and of Wang's (1G4B) and Sousa's (1G3I) doubly capped ASMS complexes are superimposed, a translation *and* a significant rotation of our HslU particles are required to superimpose them with their counterparts in the ASMS complexes. Starting from DIMS and ASMS complexes with superimposed HslV components, the HslU particles of DIMS have to be rotated by 8.2° around the local sixfold axis before they can be mapped into the HslU particles of 1G4B by a simple translation. Similarly, a 7.2° rotation and a translation of HslU are required to map DIMS into Sousa's 1G3I complex (Sousa *et al.*, 2000). This requirement for a rotation appears to have been overlooked by Wang. It also shows that different quaternary arrangements of HslV and HslU are possible (a rotation of 8° corresponds to a shift by 7 Å in the periphery of HslV). This probably accounts for the weakness of the complex and the robustness of the functional interaction against mutations (Song *et al.*, 2000).

Finally, we noticed that a weak molecular replacement solution for ASMS in P3 corresponds to the packing suggested by Wang with $U_6V_6V_6U_6$ particles at (1/3, 2/3, −1/4) and (2/3, 1/3, 1/4). The weak signal for this solution is due to HslV self- and cross-vectors that are identical to the vectors for the correct packing. Wang apparently did not notice that this solution is ruled out not only by comparison with the solution for DIMS (see above), but also due to severe molecule overlap (about 10 Å, data not shown). The suggested ASMS packing in P321 is finally ruled out by the prohibitively high *R* factor of 48% after bulk solvent correction (Wang, 2001) and by the experiments described above.

CONCLUSION

In summary, we provide support for the validity of our original analysis and interpretation of the quaternary arrangement of HslV and HslU in our cocrystals. We conclude that we did not commit any of the errors listed by Wang and prove that his reinterpretation is false by all crystallographic criteria available to him. We regret that we did not have the opportunity for a side-by-side answer to Wang.

The authors thank S. Gražulis for independently repeating and confirming a part of the calculations presented. Intensities for 1E94 as evaluated in P3 and the mercury data have been appended to PDB-entry 1E94.

REFERENCES

Bochtler, M., Ditzel, L., Groll, M., and Huber, R. (1997) Crystal structure of heat shock locus V (HslV) from *Escherichia coli*. *Proc. Natl. Acad. Sci. USA* **94,** 6070–6074.

Bochtler, M., Hartmann, C., Song, H. K., Bourenkov, G. P., Bartunik, H. D., and Huber, R. (2000) The structures of HsIU and the ATP-dependent protease HsIU–HsIV. *Nature* **403,** 800–805.

CCP4. (1994) The CCP4 suite: Programs for crystallography. *Acta Crystallogr.* **D50,** 760–763.

Crowther, R. A., and Blow, D. M. (1967) A method of positioning a known molecule in an unknown crystal structure. *Acta Crystallogr.* **23,** 544–548.

Esnouf, R. M. (1999) Further additions to MolScript version 1.4, including reading and contouring of electron-density maps. *Acta Crystallogr.* **D55,** 938–940.

Ishikawa, T., Maurizi, M. R., Belnap, D., and Steven, A. C. (2000) Docking of components in a bacterial complex. *Nature* **408,** 667–668.

Merrit, E. A., and Bacon, D. J. (1997) Photorealistic molecular graphics. *Methods Enzymol.* **277,** 505–524.

Missiakas, D., Schwager, F., Betton, J. M., Georgopoulos, C., and Raina, S. (1996) Identification and characterization of HsIV HsIU (ClpQ ClpY) proteins involved in overall proteolysis of misfolded proteins in *Escherichia coli*. *EMBO J.* **15,** 6899–6909.

Nicholls, A. (1992) GRASP: Graphical Representation and Analysis of Surface Properties. Columbia University, New York.

Otwinowski, Z., and Minor, W. (1997) Processing of X-ray diffraction data collected in oscillation mode. *Methods Enzymol.* **276,** 307–326.

Rohrwild, M., Coux, O., Huang, H. C., Moerschell, R. P., Yoo, S. J., Seol, J. H., Chung, C. H., and Goldberg, A. L. (1996) HslV–HslU: A novel ATP-dependent protease complex in *Escherichia coli* related to the eukaryotic proteasome. *Proc. Natl. Acad. Sci. USA* **93,** 5808–5813.

Rohrwild, M., Pfeifer, G., Santarius, U., Muller, S. A., Huang, H. C., Engel, A., Baumeister, W., and Goldberg, A. L. (1997)

The ATP-dependent HslVU protease from *Escherichia coli* is a four-ring structure resembling the proteasome. *Nat. Struct. Biol.* **4,** 133–139.

Song, H. K., Hartmann, C., Ramachandran, R., Bochtler, M., Behrendt, R., Moroder, L., and Huber, R. (2000) Mutational studies on HslU and its docking mode with HslV. *Proc. Natl. Acad. Sci. USA* **97,** 14103–14108.

Sousa, M. C., Trame, C. B., Tsuruta, H., Wilbanks, S. M., Reddy, V. S., and McKay, D. B. (2000) Crystal and solution structures of an HslUV protease-chaperone complex. *Cell* **103,** 633–643.

Wang, J. (2001) A corrected quaternary arrangement of the peptidase HslV and ATPase HslU in a cocrystal structure. *J. Struct. Biol.* **134,** 15–24.

Wang, J., Song, J. J., Franklin, M. C., Kamtekar, S., Im, Y. J., Rho, S. H., Seong, I. S., Lee, C. S., Chung, C. H., and Eom, S. H. (2001) Crystal structures of the HslVU peptidase-ATPase complex reveal an ATP-dependent proteolysis mechanism. *Structure* **9,** 177–184.

Yeates, T. O. (1997) Detecting and overcoming crystal twinning. *Methods Enzymol.* **276,** 344–358.